NASA/TM–2017-219611

Autonomous Inspection of Electrical Transmission Structures with Airborne UV Sensors
NASA Report on Dominion Virginia Power Flights of November 2016

Andrew J. Moore
Langley Research Center, Hampton, Virginia

Matthew Schubert
Analytical Mechanics Associates, Inc., Hampton, Virginia

Nicholas Rymer
National Institute of Aerospace., Hampton, Virginia

May 2017

NASA STI Program . . . in Profile

Since its founding, NASA has been dedicated to the advancement of aeronautics and space science. The NASA scientific and technical information (STI) program plays a key part in helping NASA maintain this important role.

The NASA STI program operates under the auspices of the Agency Chief Information Officer. It collects, organizes, provides for archiving, and disseminates NASA's STI. The NASA STI program provides access to the NTRS Registered and its public interface, the NASA Technical Reports Server, thus providing one of the largest collections of aeronautical and space science STI in the world. Results are published in both non-NASA channels and by NASA in the NASA STI Report Series, which includes the following report types:

- TECHNICAL PUBLICATION. Reports of completed research or a major significant phase of research that present the results of NASA Programs and include extensive data or theoretical analysis. Includes compilations of significant scientific and technical data and information deemed to be of continuing reference value. NASA counter-part of peer-reviewed formal professional papers but has less stringent limitations on manuscript length and extent of graphic presentations.

- TECHNICAL MEMORANDUM. Scientific and technical findings that are preliminary or of specialized interest, e.g., quick release reports, working papers, and bibliographies that contain minimal annotation. Does not contain extensive analysis.

- CONTRACTOR REPORT. Scientific and technical findings by NASA-sponsored contractors and grantees.

- CONFERENCE PUBLICATION. Collected papers from scientific and technical conferences, symposia, seminars, or other meetings sponsored or co-sponsored by NASA.

- SPECIAL PUBLICATION. Scientific, technical, or historical information from NASA programs, projects, and missions, often concerned with subjects having substantial public interest.

- TECHNICAL TRANSLATION. English-language translations of foreign scientific and technical material pertinent to NASA's mission.

Specialized services also include organizing and publishing research results, distributing specialized research announcements and feeds, providing information desk and personal search support, and enabling data exchange services.

For more information about the NASA STI program, see the following:

- Access the NASA STI program home page at http://www.sti.nasa.gov

- E-mail your question to help@sti.nasa.gov

- Phone the NASA STI Information Desk at 757-864-9658

- Write to:
  NASA STI Information Desk
  Mail Stop 148
  NASA Langley Research Center
  Hampton, VA 23681-2199

NASA/TM–2017-219611

Autonomous Inspection of Electrical Transmission Structures with Airborne UV Sensors NASA Report on Dominion Virginia Power Flights of November 2016

Andrew J. Moore
Langley Research Center, Hampton, Virginia

Matthew Schubert
Analytical Mechanics Associates, Inc., Hampton, Virginia

Nicholas Rymer
National Institute of Aerospace., Hampton, Virginia

May 2017

Acknowledgments

Available from:

NASA STI Program / Mail Stop 148
NASA Langley Research Center
Hampton, VA 23681-2199
Fax: 757-864-6500

Abstract

This report details test and measurement flights to demonstrate autonomous UAV inspection of high-voltage electrical transmission structures. A UAV built with commercial, off-the-shelf hardware and software, supplemented with custom sensor logging software, measured ultraviolet emissions from a test generator placed on a low-altitude substation and a medium-altitude switching tower. Since corona discharge precedes catastrophic electrical faults on high-voltage structures, detection and geolocation of ultraviolet emissions is needed to develop a UAV-based self-diagnosing power grid.

Signal readings from an onboard ultraviolet sensor were validated during flight with a commercial corona camera. Geolocation was accomplished with onboard GPS; the UAV position was logged to a local ground station and transmitted in real time to a NASA server for tracking in the national airspace.

Introduction

Manually piloted UAVs have been deployed routinely to inspect high-voltage electrical transmission lines in the past two years [1, 2, 3, 4], and a variety of sensors and concepts for autonomous transmission line inspection have been proposed (see [5, 6] for reviews). One or more manual flights to test sensors, operational concepts, and autonomy methods are needed to verify a particular UAV platform; commonly at least one manual flight within a given flight corridor is undertaken to determine inspection poses and to cope with site-specific geography. Once a site is surveyed and waypoints along an effective flight inspection corridor are determined, autonomous UAV flights can economically reinspect a line section repeatedly. The work described in this report follows in that same sequence: exploratory manual flights are followed by autonomous flights at two de-energized high-voltage infrastructure locations.

Most of the technologies described herein are broadly applicable to UAV deployment. In addition, this report describes results obtained from a compact UV sensor package developed at NASA Langley that is specifically applicable to high-voltage fault detection. In electrical power transmission, great care is taken to avoid sharp protrusions on high-voltage structures; electron avalanches from high-potential points produce, via impact ionization and subsequent recombination of atmospheric plasma, an ultraviolet (UV) photon spray called coronal discharge [14]. While most coronas are benign, some are indicative of a severe degradation that requires immediate attention; location, diagnosis, and disposition of coronas are necessary components of transmission line inspection. The core technology, a sensor based on the photoelectric effect and gas multiplication [8], is solar blind and has a wide field of view. An early version of this sensor was calibrated against a 100 kV corona [15]; subsequent versions are more sensitive, allowing a greater standoff distance from the high-voltage structure.

Since it is very lightweight, this technology can be mounted on the UAV. If the sensitivity is high enough to allow a sufficient standoff distance, a fleet of UAVs equipped with compact UV sensors could autonomously inspect high-voltage structures and locate faults that may result in a power outage. If distributed across a power grid (for example, at substations), this fleet could serve as the detection component of a self-diagnosing power grid (Figure 1). Imagery and other telemetry from the UAV deployments could then be interpreted remotely by experienced grid operation and line crews, enabling the rapid dispatch of a nearby line crew in a repair truck loaded with the components necessary to repair the fault.
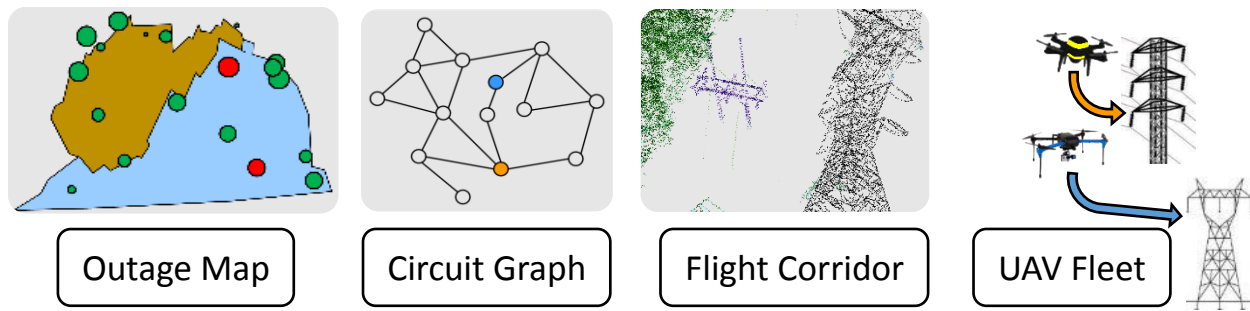
Figure 1. Components of a self-diagnosing power grid. UAVs cached at locations across the grid, such as electrical substations, can be deployed on demand to locate and characterize the faults based on geographic outage maps and topological circuit maps.

Test and Measurement Flights

Two days of experimental UAV flights were conducted at Dominion Virginia Power's Chester training facility on November 7 and 8, 2016. A variety of commercial transmission structures, de-energized for training purposes, are located at this facility. The UAV was built with commercial, off-the-shelf hardware and software, supplemented with custom sensor logging software. Twelve test flights with increasing instrumentation validated the measurement methods at two structures: a low-altitude substation, and a medium-altitude switching tower. At the site of each structure, manual flights were conducted first, in preparation for a waypoint-based autonomous flight.

A corona generator was placed on each structure, with a coronal UV intensity strength set to produce a signal measurable by a pair of onboard ultraviolet sensors. The UAV distance from the generator was no closer than 12' for manual flights, and no closer than 20' for autonomous flights. To validate sensor records, visible and ultraviolet imagery of the flight path was recorded.

UAV position was tracked by the onboard autopilot and saved to a ground computer after the flights each day. In addition, the UAV position was forwarded during the flight from the ground station computer to a NASA server for real-time traffic management. After all flight data capture and recording technologies were operating successfully, as proven in test flights, measurement flights were conducted at the two locations. These flights demonstrated, for the first time, an autonomously guided UAV with onboard compact UV sensors recording signals directly relevant to transmission line fault geolocation, while tracked in the national airspace. Selected video clips from these flights may be seen in [19].

Flight locations within the Chester training facility are shown in Figure 2. The substation is a recently added structure at the east side of the facility, and the switching tower is at the far north side, close to Old Stage Road in Chester, Virginia. The video and corona cameras were placed 200 to 300 feet from the flight locations to accommodate the small depth of field of the corona camera.

Tables 1 and 2 list the details for each flight. Test flights took place on the first day and the morning of the second day, and measurement flights took place in the afternoon of the second day. Flights are designated according to the structure, day, and flight count[1]: substation flights begin with S1_1 and end with S2_5, while tower flights begin with T1_1 and end with T2_4.

---

[1] SD_R (S=Substation, D=Day, R=Repetition) and TD_R (T=Tower, D=Day, R=Repetition)

Tables 1 and 2 are combined in an inventory of all flights in Appendix 1. Appendix 2 documents all equipment and software used in these flights.
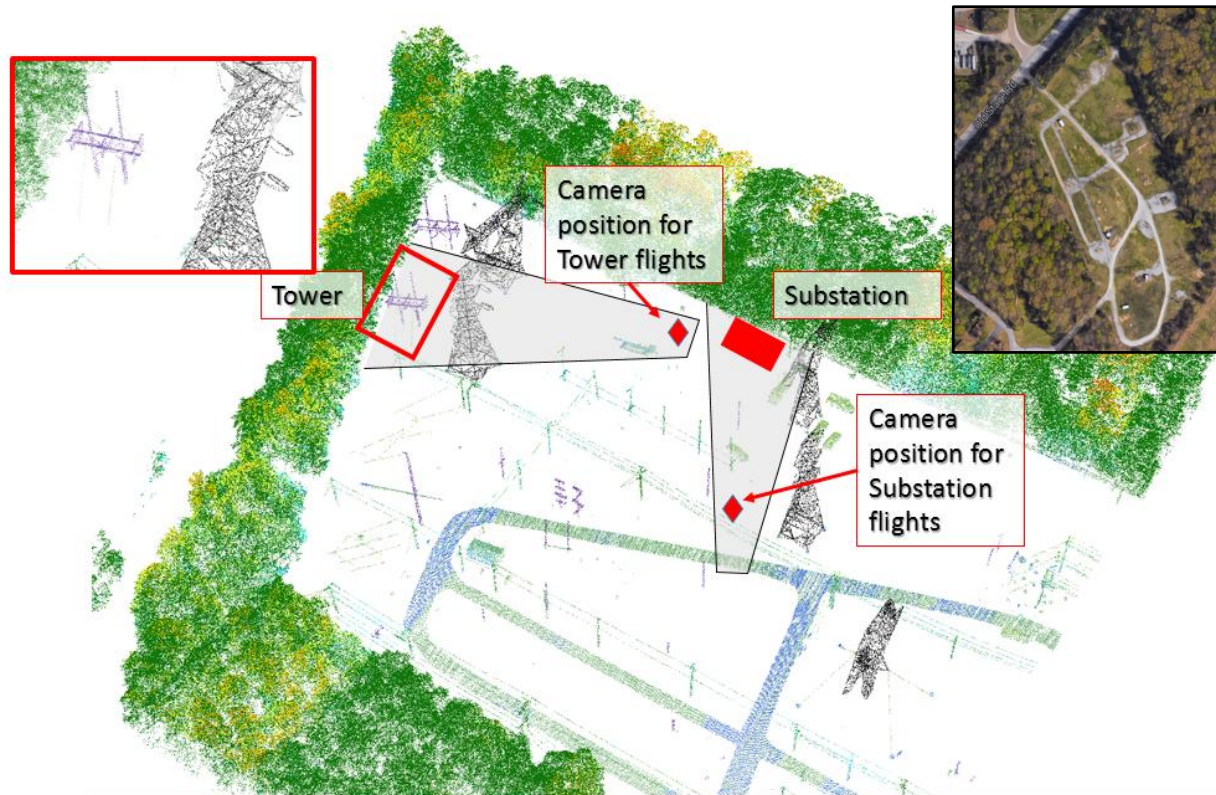

Figure 2. Chester Virginia flight range. Flight and camera positions superimposed on Dominion-provided lidar. The flight locations and camera recording positions for the substation and tower flights were in the northeast corner of the range. A close-up of the switching tower is shown in the top left inset, and a satellite image of the facility (for which up is north) is shown in the top right inset. *©Lidar data: Dominion Virginia Power; Map data: Google, DigitalGlobe & NASA*

Substation Test and Measurement Flights

Low-altitude flight maneuvers and sensor checks were accomplished in the substation (S) test flights (top of Table 1). After a free-ranging manual flight S1_1 that approached as close as 12 feet to the target location, the corona source was energized and the UV sensors were tested in autonomous flights S1_2 and S1_3, which approached as close as 20 feet to the target location. Figure 3 illustrates the physical interpretation of the UV plots in this report, using as an example L-shaped UAV flight path of test flight S1_3. Since the corona sensors were on the sides of the UAV, the left (port) sensor detected corona during the first leg, and the right (starboard) sensor detected corona during the second leg, which was ~8 feet from the concrete pad of the structure, and ~20 feet from the substation hardware. With the waypoints used in S1_2, the flight ended before the UAV made a full sweep in front of the source, and so the final waypoint was moved north for a full sensor sweep (column 'UV Plot' of Figure 4).

This result was verified in a back-and-forth manual flight in front of the substation (S2_1). The UAV was kept oriented approximately north so that it was flying forward and then backward multiple times; several peaks of signal strength (which correspond to points of nearest approach) are seen from the right sensor. Additionally, the UAV flight path was transmitted to a remote NASA UAS Traffic Management (UTM, reference [7]) server during this flight.

Finally, corona camera recording and UTM flight path transmission was conducted in the trio of measurement flights S2_3, S2_4, and S2_5 (Figure 5 and bottom of Table 1)[2]. The UAV altitude was varied in these three flights so as to frame it in the limited field of view of the corona camera. Altitudes of 9.8 feet (3 meters; flight S2_3) and 16.4 feet (5 meters; flight S2_4) were too low and too high, respectively, to capture the UAV within the corona camera frame, but an altitude of 13.1 feet (4 meters; flight S2_5) produced corona camera video imagery that independently validated the corona signal detected by the onboard sensor (Figure 6).

Even at low altitude, the S2_5 measurement flight was a necessary validation of the methodology, and upon success it was justifiable to proceed with a higher altitude measurement at the switching tower site. While corona detection at altitudes above 30 feet is required for broad applicability of the technique, the substation test and measurement flights sufficed to show that all of the basic principles were sound and that all of the measurement methods were producing valid results.
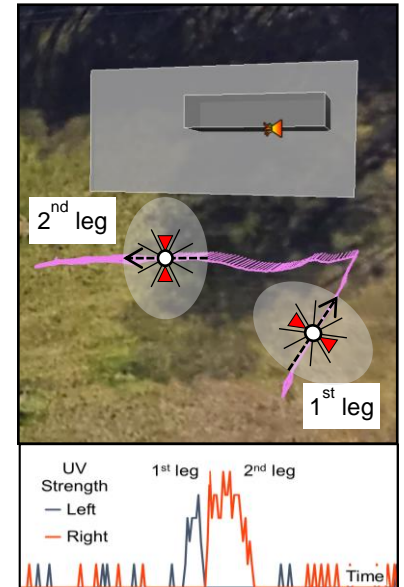

Figure 3. Spatial validation of the signals from port (left) and starboard (right) compact UV sensors ©*Map data: Google, DigitalGlobe & NASA*

Table 1. Substation test and measurement flights

Substation Test Flights								
Date	Flight	Description	UV Plot	Flight path	UV Image	Visible Image	UTM path	UTM boundary
Monday, Nov 7	S1_1	1st manual flight		✓				
	S1_2	1st auton. flight	✓	✓		✓		
	S1_3	2nd auton. flight	✓	✓		✓		
Tuesday, Nov 8	S2_1	1st manual flight	✓	✓		✓	✓	
Substation Measurement Flights								
Date	Flight	Description	UV Plot	Flight path	UV Image	Visible Image	UTM path	UTM boundary
Tuesday, Nov 8	S2_3	2nd auton. flight		✓			✓	
	S2_4	3rd auton. flight	✓	✓			✓	
	S2_5	4th auton. flight	✓	✓	✓	✓	✓	✓

---

[2] Flight S2_2 was aborted and no useful data resulted. Although listed in the flight inventories in the appendices, it is not described further. Onboard sensor data was not obtained for flights S1_1 and S2_3.

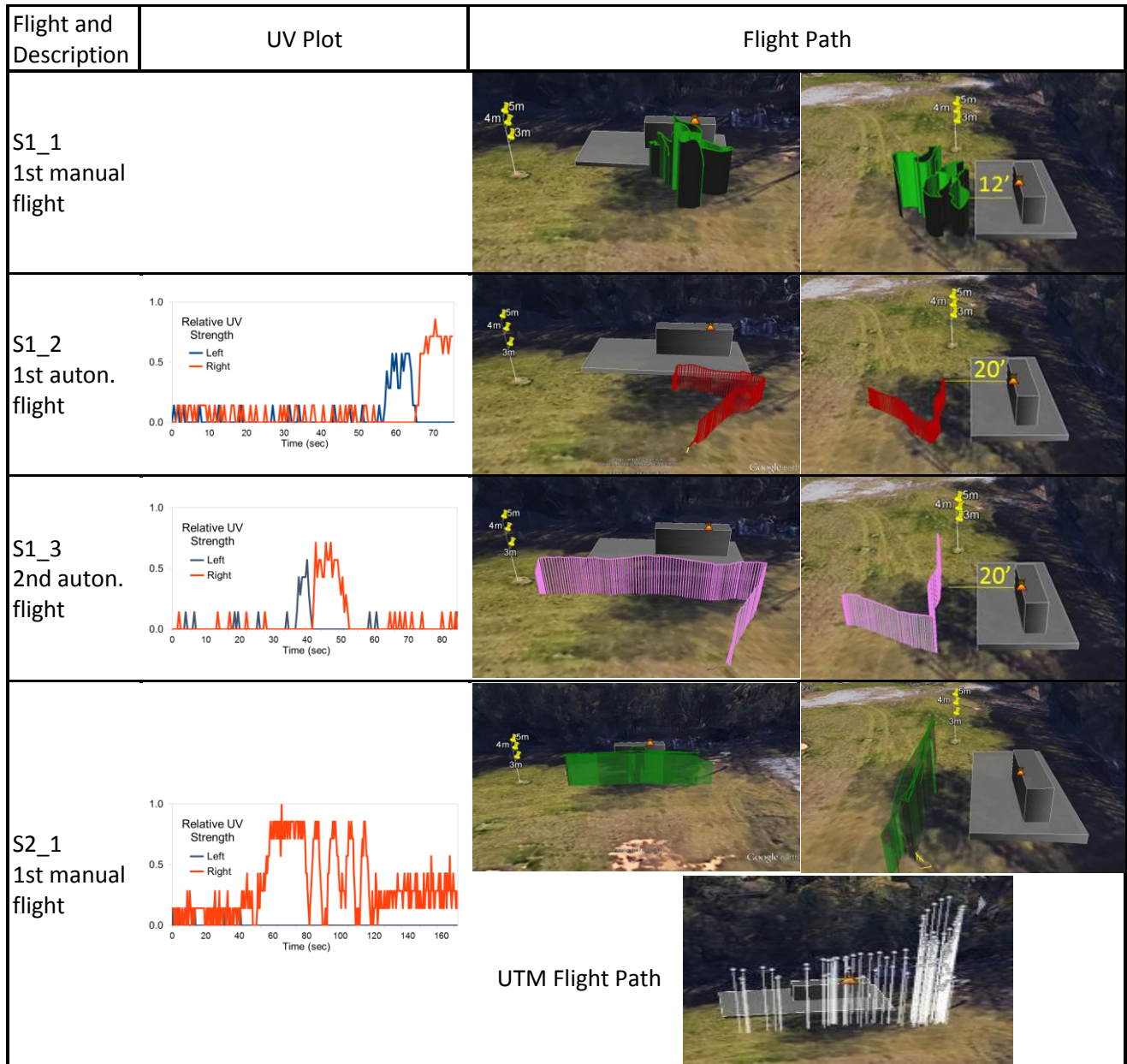| Flight and Description	UV Plot	Flight Path
S1_1 1st manual flight		
S1_2 1st auton. flight		
S1_3 2nd auton. flight		
S2_1 1st manual flight		 UTM Flight Path

Figure 4. UV signal and flight path plots for the four substation test flights. The approximate distance to the corona generator (12' or 20') is indicated for the first three flights, which verified the compact UV sensor response. For the final test flight, the flight path was transmitted to the NASA UAS Traffic Management (UTM) server, and is shown at the bottom right for flight S2_1. *©Map data: Google, DigitalGlobe & NASA*
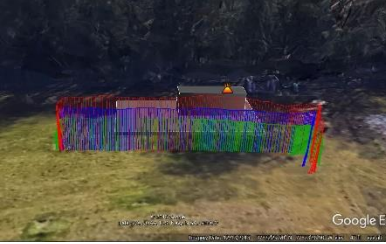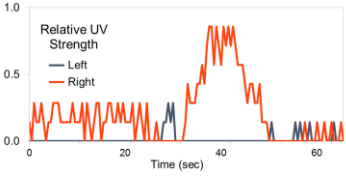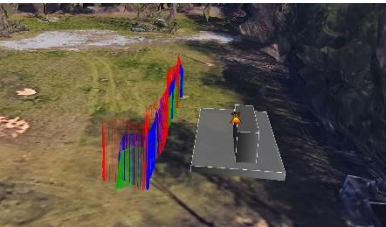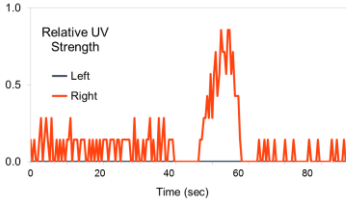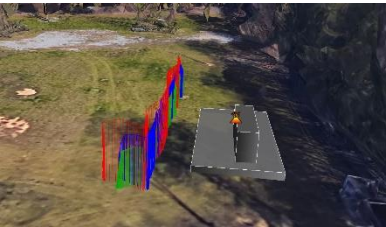
Flight	Altitude (m)	UV Plot	Autopilot Flight Paths (overlay)	UTM Flight Path
S2_3	3	(not recorded)		
S2_4	5			
S2_5	4			

Figure 5. Altitude, UV signal and flight path plots for the three substation measurement flights. Both autopilot and UTM flight paths are shown; autopilot flight paths for all three flights are overlaid in the center column, showing flight paths with three altitudes (3, 5, and 4 meters colored green, red, and blue) in frontal and lateral views. The UTM flight paths (right column) are shown individually for each flight in frontal view. Note the altitude errors in the UTM plots; please see the section *Altitude reporting in autopilot and UTM records* below for a discussion of the origin of these errors and alternative altitude measures. ©*Map data: Google, DigitalGlobe & NASA*

Figure 6. Validation of the compact UV sensor signal with corona camera in a substation measurement flight. The visible camera image shows the UAV above the substation structure (background; UAV is in lightened ellipse). The inset at top right shows the compact UV sensor recording, which reaches a maximum as the UAV passes the corona generator. The inset at bottom right shows the corona camera record; the bright red blobs at the center of the image are locations of UV emission.

Switching Tower Test and Measurement Flights

Medium-altitude flight maneuvers and sensor checks were accomplished in the tower (T) test flights (top of Table 2; Figure 7)[3]. A back-and-forth manual flight with increasing altitude (T1_1) was executed to frame the UAV in the corona camera's field of view and to set waypoints for an autonomous flight. In two subsequent autonomous flights on day 1 (T1_3 and T1_4), the UAV failed to detect an ultraviolet signal and drifted off of the planned flight path halfway between the waypoints. The detection failure was due to a poor contact between the corona generator's body and its emitting tip.

Work at the switching tower resumed in the afternoon of day 2, after a newer corona generator (with a solid contact) was placed aloft in the morning. A manual flight (T2_1) was executed first to frame the UAV and corona generator in the corona camera view and to establish waypoints. As in day 1, just two waypoints were used, one to the west and one to east of the tower. Flight from east to west (flight T2_4)[4] proceeded along the planned flight path.

---

[3] Three flights (T1_2, T2_2, and T2_3) were aborted and no useful data resulted. Although listed in the flight inventories in the appendices, they are not described further.

[4] Two attempts to fly autonomously from west to east failed (T2_2 and T2_3, not shown in Figure 6), because the pilot aborted the flight after the UAV drifted south, off of the intended flight path. We speculate that the GPS signal was erratic at the west waypoint, situated between the switching tower and a nearby tall steel lattice tower,

All experimental datatypes were captured in measurement flight T2_4 (Figure 8): onboard UV sensors recorded the generated corona as verified with the ground-based corona camera (Figure 8), and the UAV flight path was transmitted to a remote NASA UTM server (bottom right of Figure 8; Figure 10). Success at the altitude of the switching tower confirmed the practicality of the UAV-based method for corona inspection of transmission line infrastructure.

It is critical to note that confirmation of practicality is not sufficient to prove adequacy. We estimate that the onboard sensor used in these experiments is capable of detecting corona of a magnitude produced by an actual 100 kV corona fault at a distance of 12 feet. However, the magnitude of the artificial corona source used was set higher than that of a 100 kV corona, so that detection could be tested at greater distances. Until the method is verified on actual corona faults, we cannot state with certainty that the technologies tested in this study will produce diagnostic results. Thus we can claim that the method has practicality and relevance, but not adequacy, until it is tested successfully on a calibrated UV source or an actual fault.

In summary, these flights demonstrated, for the first time, an autonomously guided UAV with onboard compact UV sensors recording signals relevant to transmission line fault geolocation, while tracked in the national airspace.

Table 2. Tower test and measurement flights

Tower Test Flights								
Date	Flight	Description	UV Plot	Flight path	UV Image	Visible Image	UTM path	UTM boundary
Monday, Nov 7	T1_1	1st manual flight		✓				
	T1_3	2nd auton. flight, aborted into alt hold	X	✓				
	T1_4	3rd auton. flight, aborted into alt hold	X	✓				
Tuesday, Nov 8	T2_1	1st manual flight		✓				
Tower Measurement Flights								
Location	Flight	Description	UV Plot	Flight path	UV Image	Visible Image	UTM path	UTM boundary
Tuesday, Nov 8	T2_4	3rd auton. flight	✓	✓	✓	✓	✓	✓

---

while the GPS signal was stable at the east waypoint, which is comparatively further from a second nearby steel lattice tower.
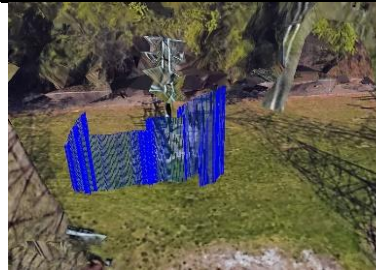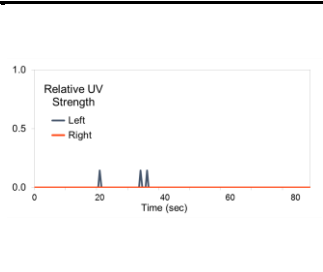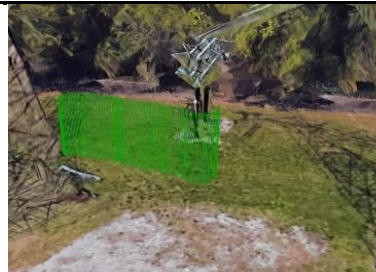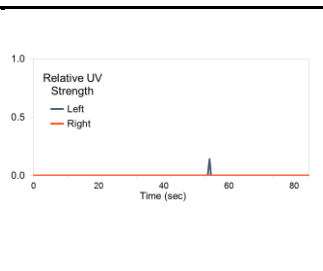
Flight and Description	UV Plot	Autopilot Flight Path	
T1_1 1st manual flight			
T1_3 2nd auton. flight			
T1_4 3rd auton. flight			
T2_1 1st manual flight			

Figure 7. UV signal plot and autopilot flight path for the tower test flights. As with the substation flights, the standoff distance is 12' for manual flights and 20' for autonomous flights. The outputs from the compact UV sensor, recorded in the autonomous flights, show no signal, due to a corona generator malfunction. *©Map data: Google, DigitalGlobe & NASA*

Flight and Description	UV Plot	Flight Path
T2_4 2nd auton. flight		 UTM Flight Path
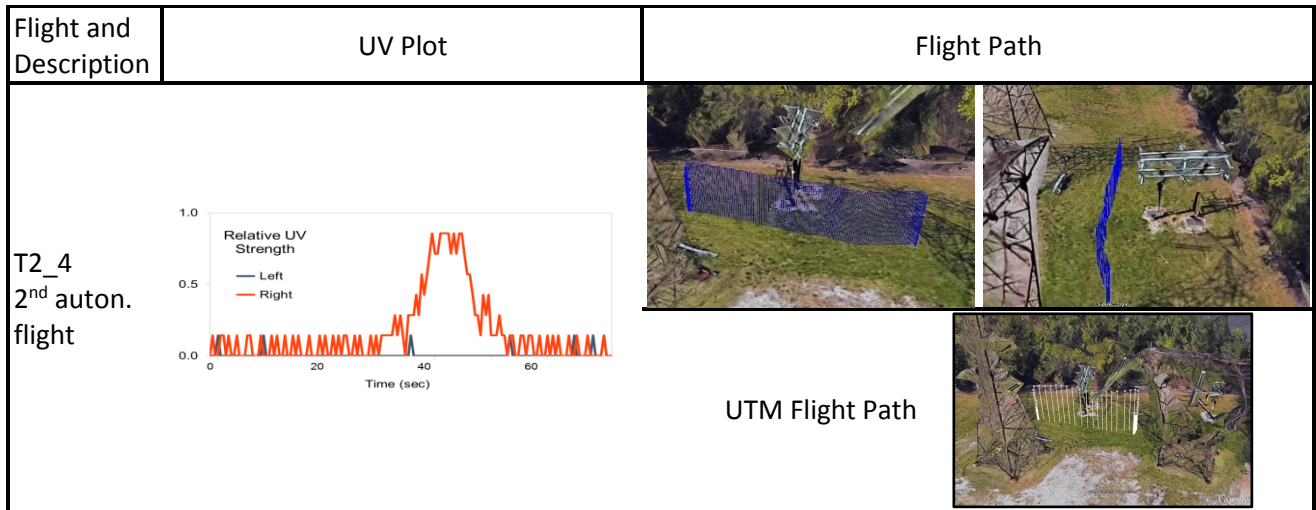
Figure 8. UV signal plot and autopilot flight path for the tower measurement flight T2_4. The compact UV sensor records a signal as the UAV passes the corona generator. Both autopilot (top right) and UTM (bottom right) flight paths are shown. *©Map data: Google, DigitalGlobe & NASA*
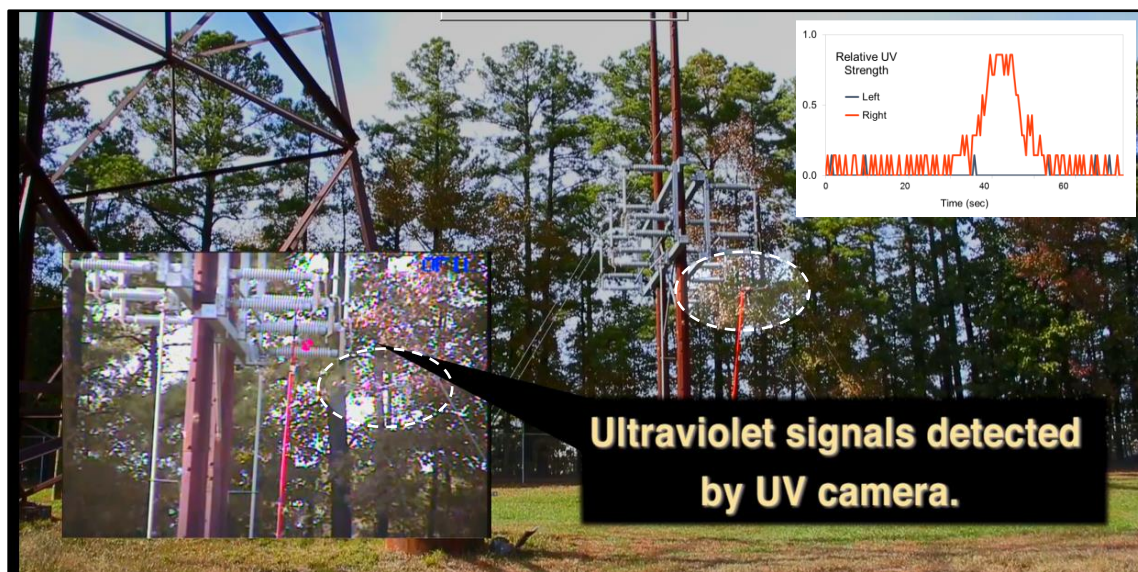
Figure 9. Validation of the compact UV sensor signal with corona camera in tower measurement flight T2_4. The corona camera imagery (inset at left) verifies the UV sensor result (inset at top right). The UAV is framed in a low-contrast oval (white dashed outline) in this imagery. The bright red blobs at the center of the corona camera image are locations of UV emission.
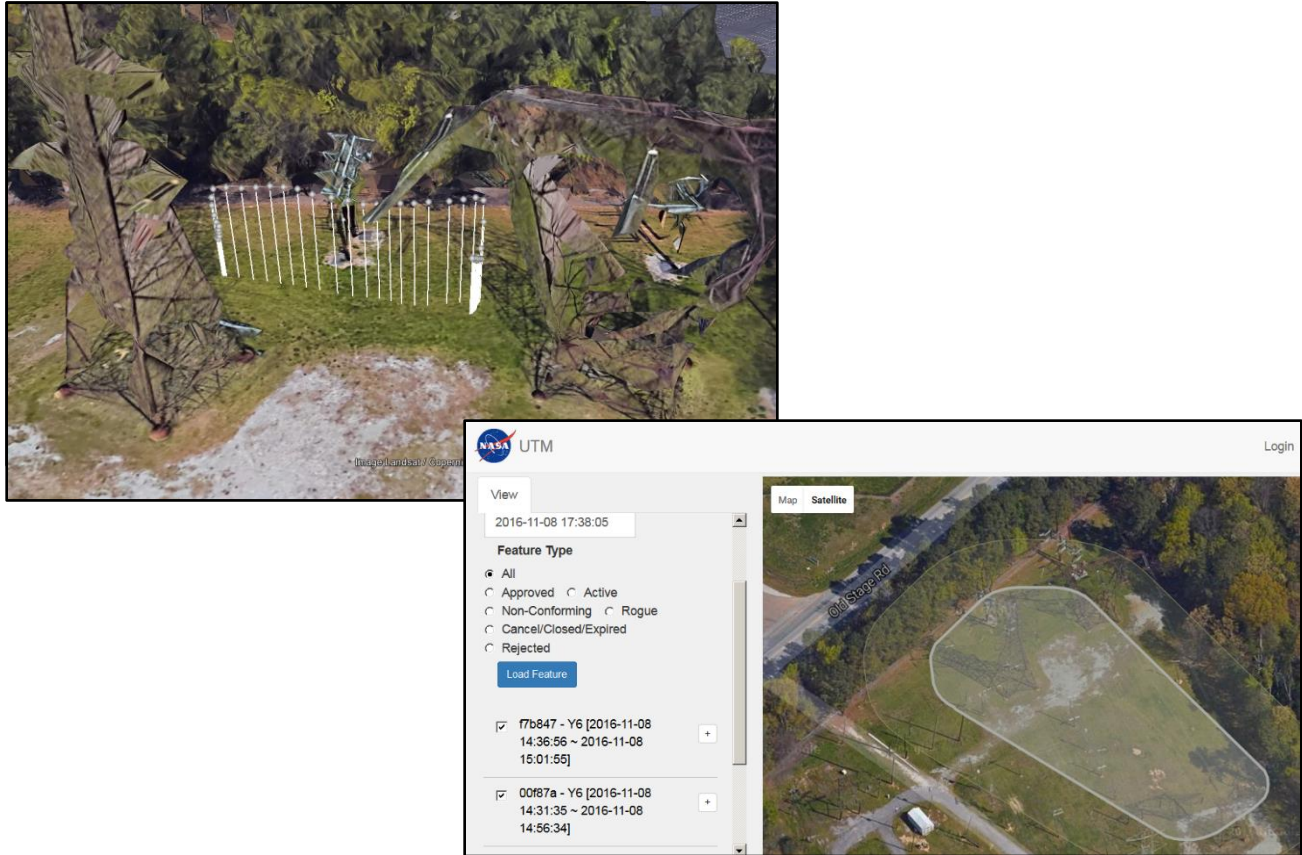
Figure 10. UTM flight path and UTM boundary and buffer ring for measurement flight T2_4. (Note: the boundary extends to the south due to a stale home position retained by the autopilot from the substation measurement flights earlier in the day.) The UTM path and boundary are the representations used to track the UAV flight in the national airspace. *©Map data: Google, DigitalGlobe & NASA*

Discussion

Compact sensor technology and standoff distance

The UAV was built with commercial, off-the-shelf hardware and software, supplemented with custom sensor logging software. The base aircraft platform cost was less than $5K, and commercial laptops were used as ground stations.

One consequence of this low-cost approach is that UAV positional accuracy is too low to allow precision autonomous flights. The test signal was increased to compensate for this deficiency. In this section, the experimental approach and caveats about interpretation of the results are detailed.

Leveraging new sensor and UAV technology development

Compact UV sensors promise to supplement or replace corona cameras for finding potential high-voltage transmission line faults [1]. Corona camera adoption is limited, at least in part, due to camera size, cost, and fragility; compact UV sensor technology is superior in all three of

14

these measures of market fitness. However, corona cameras have exquisite sensitivity to the weak UV photon flux density produced by coronas. They are so sensitive that a user with limited training can spot a corona from the ground at a distance of 300 feet or more. In contrast, compact UV sensors must be located within a few yards of a corona to sense it reliably.

As a result, compact UV sensors have not been applied in transmission line inspection. Two recent technology advances may change this: an increased sensor sensitivity, and the broad deployment of UAVs that can deliver the sensor very close to the corona source.

Device sensitivity and range

Figure 11 shows the improvement in sensitivity of a commercial line of UV sensors [18] that use the photoelectric effect to sense narrow-band UV photons in a Geiger-Mueller tube and circuit configuration. The leftmost model was calibrated experimentally at the Electric Power Research Institute in July of 2015 to determine detectability of a 100 kV corona [15]. The device (R9533, left device in Figure 11) has to be within four feet of the discharge to reliably report a signal corresponding to a 100 kV corona (four foot maximum detection distance). Its successor (R1753-01, middle device in Figure 11) is twice as sensitive in our laboratory tests (eight foot maximum detection distance from a 100 kV corona). In 2016, a new design (R13192, right device in Figure 11) yielded an additional 50% higher sensitivity (twelve foot maximum detection distance from a 100 kV corona).

In our laboratory tests of the third generation device (Figure 12), a commercial corona generator (Electro-Technic Products BD-20A High Frequency Generator) was energized to approximate a 100 kV corona, and a signal was detected at a distance of sixteen feet. This exceeds the expected maximum detection distance of twelve feet. This discrepancy was likely due to a laboratory corona generator setting that produces more UV flux than a 100 kV corona; the depth axis in Figure 12 is scaled by 0.75 to correct this calibration error.

The devices from each generation have a very wide (>90°) field of view. There are two methods to enhance the sensor range, but both add cost and weight and decrease the field of view. First, optical focusing with a UV-transparent lens approximately doubles the detection distance [11, 12]. However, the quartz lenses are heavy and cost much more than the sensor, and the field of view for practical lenses is limited to about 10 degrees. Second, optical focusing with a UV-reflective mirror can increase the detection distance by a factor dependent on the mirror radius and curvature [9, 10]. Such a mirror will add weight and cost, but the field of view can still exceed 90 degrees [9].
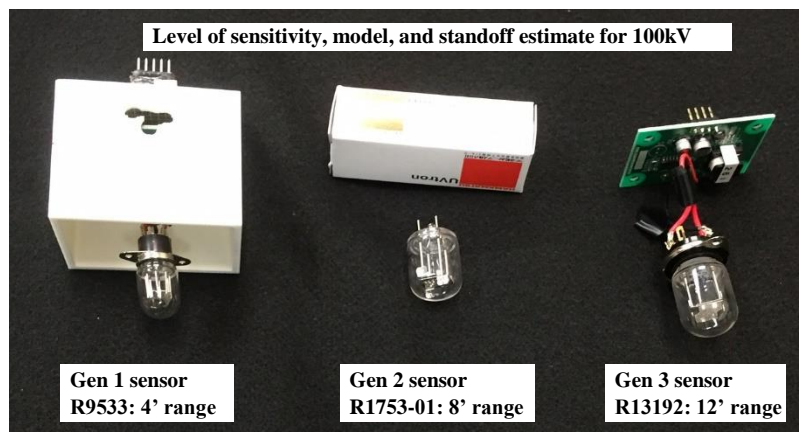

Figure 11. Left: The Hamamatsu line of compact UV sensors from the first generation, which can sense a 100kV corona at four feet of standoff, to the third generation (R13192), which can sense a 100 kV corona at a distance of approximately twelve feet.

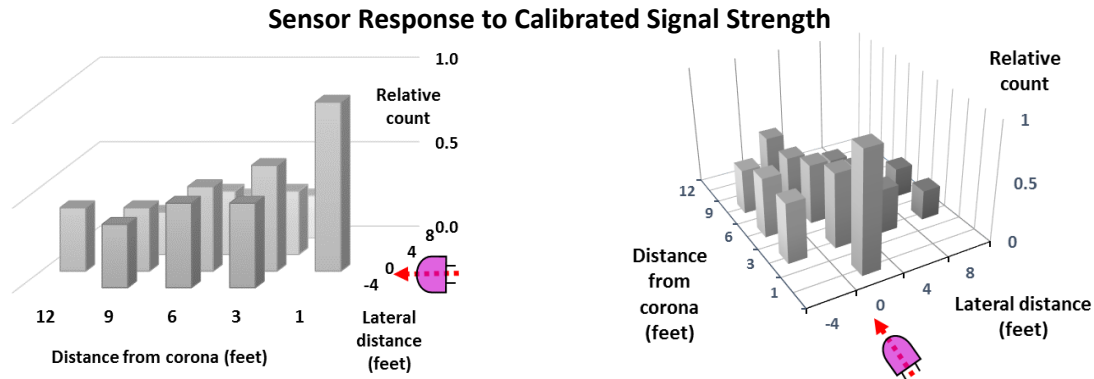**Sensor Response to Calibrated Signal Strength**

Figure 12. Sensitivity profile of the R13192 photoelectric UV sensor, with the corona generator set to approximate a 100 kV corona. At left is a top oblique view of the profile, and at right is a moderately elevated side view. The sensor location is indicated by the arrow and bulb icon.

Airborne Standoff Distance and Corona Generator Settings

For brevity, we use sGPS to indicate single-ended GPS, and dGPS to indicate differential GPS [16] in this report.

To achieve adequate sensing, a UAV equipped with a third generation photoelectric UV sensor must carry it to a distance of 12 feet or less from the source of 100 kV corona emission. This can be achieved safely for manual flight (i.e., using the joysticks on an RC transmitter) if the pilot continuously controls the standoff distance. For autonomous flights, GPS or other geolocation methods are needed to enforce standoff.

Twelve feet is only slightly greater than the accuracy of standard, consumer-grade sGPS. GPS accuracy is a statistical quantity, meaningful only for a percentage of measurements. Using 95% as the statistical allowance, sGPS accuracy is about six feet in latitude and longitude and approximately 2 times poorer in altitude accuracy [17]. UAV autopilots commonly use a barometer for altitude correction of sGPS. Figure 13 illustrates this challenge: inexpensive sGPS introduces an envelope of positional uncertainty around the UAV that is a large fraction of the corridor volume needed for accurate measurement.
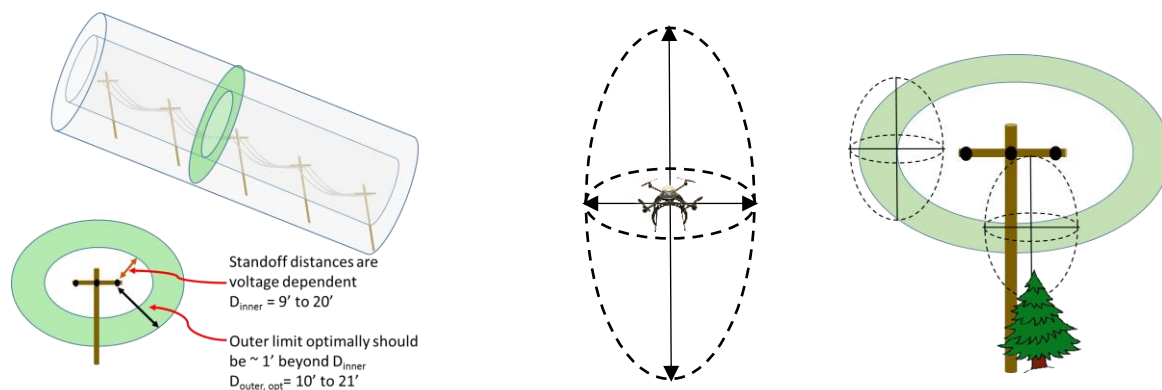

Figure 13. Flight volume (left), positional uncertainty (middle), and sensing pose (right). With single-ended GPS, the positional uncertainty is a large fraction of the desired standoff distance.

An increase in accuracy is possible with differential GPS (dGPS), in which two single-ended receivers, one on the UAV and another on the ground station, compute a relative location. When operating with full fidelity, dGPS has a positional uncertainty on the order of centimeters. We pursued this technology throughout 2016. Our research confirmed that dGPS can, in the best case, deliver this accuracy, but that this ideal level of fidelity was intermittent.

For example, when not attached to a UAV, full accuracy was possible, but when mounted on the aircraft it was rare. In fact, the autopilot that we used (Pixhawk controller [13], running Arducopter 3.3) will not allow arming and takeoff of a UAV if dGPS accuracy is poor, and we could never achieve the required accuracy for arming and takeoff with dGPS guidance.

Over the course of the year, two other NASA research groups attempted to adopt low-cost dGPS technology with varied success. Significantly, if arming and takeoff were successful and dGPS "lost lock" (i.e., failed to meet a threshold level of accuracy) during the flight, the autopilot would shift to an onboard backup single-ended sGPS. When this shift occurred, the spatial control envelope of the UAV would expand from centimeters to meters, and the aircraft would jump into a new position estimated from the (low accuracy) single-ended sGPS. This jump, while not catastrophic a) is jarring and can lead to pilot overreaction, and b) almost always resulted in a mission abort due to autopilot safety protocols. At present, the level of confidence in dGPS units small enough to fly on a UAV is very low. To obtain NASA flight safety permissions for the Chester flights, we had to remove differential GPS from the research program, because of concerns about sudden loss of control.

To compensate for this, we increased standoff distance for autonomous flights from 12 to 20 feet (Figure 14). At a twenty foot standoff distance, even a shift of six feet (from the center to the outer limit of the positional accuracy envelope) would not result in a collision of the UAV into the inspected structure. The corona generator output had to be increased above the 100 kV
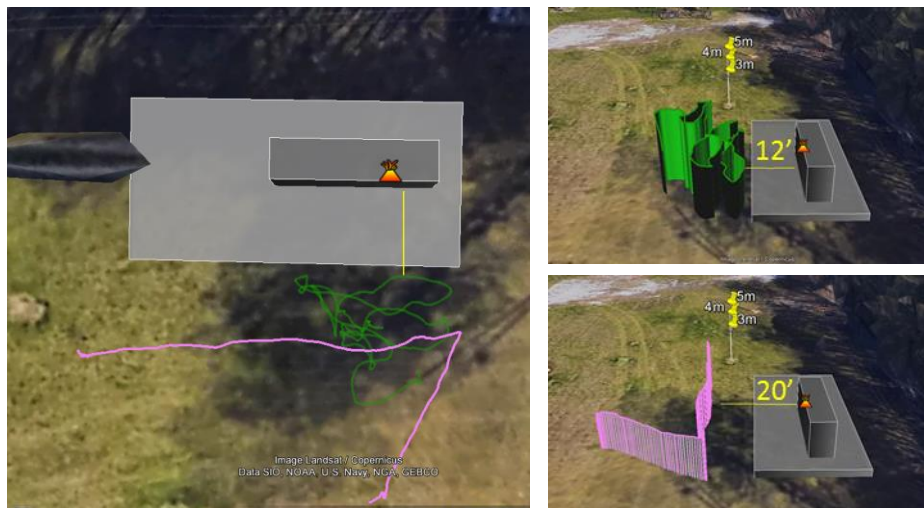
Figure 14. Distance from corona source in manual and autonomous flights. Top and side views for flights S1_1 (green) and S1_3 (pink) are shown. Due to GPS uncertainty, while manual flights approached the 12 foot calibration distance, autonomous flights approached no closer than 20 feet (horizontal yellow line). To compensate, the corona generator output was increased above calibration levels. *©Map data: Google, DigitalGlobe & NASA*

calibration output level to be detectable at a 20 foot distance. This is why we emphasize the following caveat: until the method described in this report is verified on actual corona faults, we cannot state with certainty that the technologies tested in this study will produce diagnostic results. We can claim that the method has practicality and relevance, but not adequacy, until it

is tested successfully on a calibrated UV source or an actual fault. Improved positional accuracy is critical to proving adequacy.

Using only sGPS positional accuracy as a guide, we can conclude (right image of Figure 13) that flying beneath power lines is not safe, and that flying to the side (as done in this study) is safe but not adequate. Flying over lines using sGPS for navigation is safe, but adequacy is even more problematic because sGPS vertical positional uncertainty is 2X greater than sGPS horizontal positional uncertainty. If the vertical positional uncertainty can be reduced, then flying over lines or above and to the side of them is possible (Figure 15). We did not thoroughly quantify the accuracy of the autopilot's fusion of sGPS and barometer, but the results from flights S2_3, S2_4, and S2_5 indicate that the required vertical accuracy is already available. Currently available low-cost laser altimeters are rated at ± 0.3 ft (10 cm) at 16.4 ft (5 m) and higher altitudes. An example flight geometry with these assumptions is provided in Appendix 3.
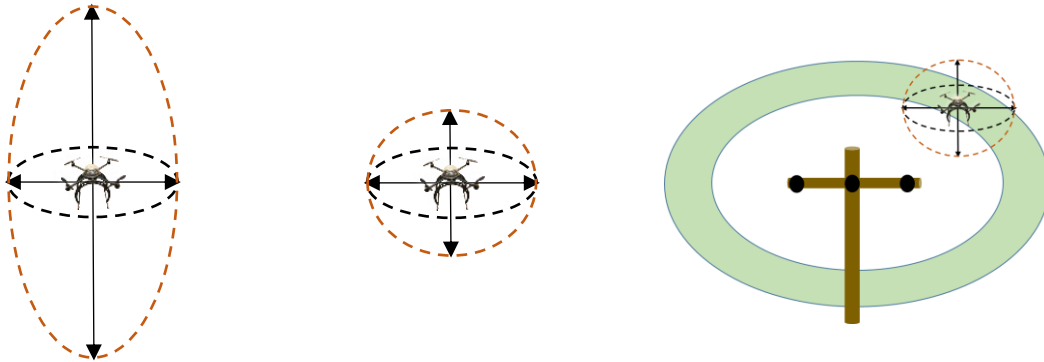

Figure 15. Reducing vertical position uncertainty. Left: sGPS uncertainty. Middle: Barometric or laser altimeter correction of vertical position estimate, fused with sGPS horizontal position estimate. Right: An example safe position that results from improved vertical accuracy.

Altitude reporting in autopilot and UTM records

Merging and reconciling the multiple data types gathered in these experiments was demanding due to the data volume, but not difficult, with one exception. The UAV autopilot forms altitude estimates from barometric, inertial, and sGPS/dGPS sensors, and from combinations of these. The estimates are computed relative to ground, relative to takeoff altitude and relative to a fixed datum, e.g., sea level. Reconciling the observed and recorded altitudes required a survey of all of these computed altitudes, trying each on our mapping tool (Google Earth). To render sensible flight paths, custom processing was needed to substitute a stable altitude record prior to mapping, because the default record is subject to profound drift as shown in Figure 16. A beneficial advance that emerged from this study is the discovery that the UTM record, which uses the error-prone default, can be improved with the same simple substitution.
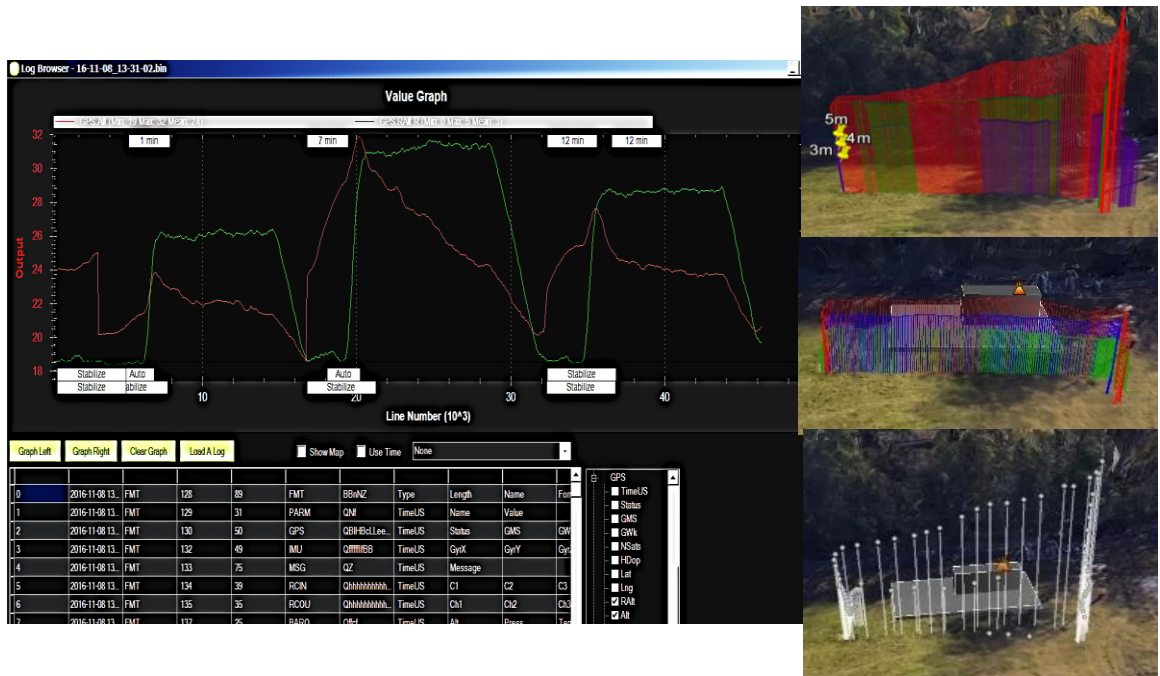
Figure 16. Altitude reporting among data types. Data is shown for flights S2_3, S2_4, and S2_5, with known altitudes of 9.8 ft, 13.1 ft, and 16.4 ft, (3m, 5m, and 4m), respectively. In this autonomous flight series, the UAV flew from south to north, which is from right to left in the views shown. The default UAV altitude is subject to profound drift (red trace at left), but a stable form is available in the logs (green trace). At right are the flight paths using the two forms: top, the default autopilot log; middle, corrected autopilot log; bottom, UTM record. The UTM stream would benefit from substitution of the corrected altitude.

Advancements for repeated autonomous flights

Multiple technology developments are required to advance from current manual flights to a self-diagnosing grid. In this section, we discuss the outlook for two of them: UAV location determination and compact fault sensing.

Improving positional accuracy

One technology gap that prevents autonomous UAV inspection flights is positional accuracy. Both sGPS and dGPS cannot close the gap, in our view. As discussed above, single-ended GPS is not accurate enough to approach a 100 kV corona close enough to measure its UV emission with current compact sensors. The two low-cost differential GPS systems that we tested are small enough to fly on an under-55-lb UAV, but fail intermittently; this can result in abrupt position changes during the UAV flight.

A long-term goal of UAV research is autonomous navigation in a GPS-denied environment, so success without these hindrances would have only been provisional. Location of the UAV via sGPS/dGPS is a transitional goal until solid alternatives become available. As a location technology, sGPS/dGPS inaccuracy presents obstacles to safe (contactless) UAV-based infrastructure inspection that can be mitigated as follows.

Some possible strategies to advance autonomous measurement adequacy given GPS uncertainty are:

1. Use autonomous flight segments whenever possible to safely approach the transmission structure, supplemented with manual flights as needed
2. Equip the UAV with reliable (presumably high-cost) differential GPS, or develop diagnostics that alert the pilot if high-accuracy flight is not available
3. Develop alternative positioning technology such as lidar, sonar, radar or stereo vision

1. Autonomous vs. manual flights and safe separation

In manual flights, standoff distances adequate for UV sensing is attainable if a pilot has a good view of the UAV standoff from the inspection structure. In all flights described in this report, the pilot position was chosen to ensure a good view. We designed autonomous flight paths (i.e., waypoints) sufficient for successful inspection without manual pilot intervention. Due to the horizontal positional uncertainty (95% confidence level) of single-ended GPS (Figure 13), we were forced to adopt a conservative and inadequate horizontal standoff distance for autonomous flights (Figure 14).

Flights above (rather than to the side of) inspection structures can take advantage of the smaller vertical uncertainty afforded by non-GPS altimetry (Figure 15). Specific examples are shown in Figure 17. The placement of static wires, which are sometimes poorly resolved in lidar imagery, is an important constraint to consider in developing this approach.
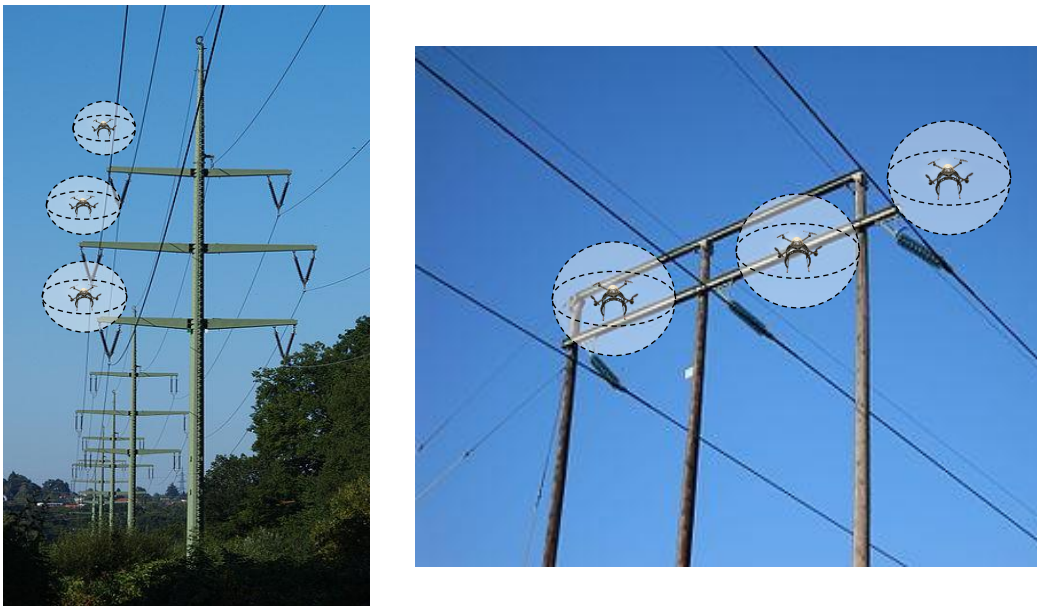
Figure 17. Examples of inspection positions that take advantage of reduced vertical uncertainty

2. Invest in more accurate GPS or diagnostics

We tested two hobby-grade differential GPS systems that cost $1000 or less, and avoided more mature systems that cost $5000 or more, since those systems cost more than the UAV itself. High-grade differential GPS packages may offer greater stability and uptime than the two packages we tested.

In the future, low-cost, compact systems can in principle be supplemented with diagnostics that indicate whether precision flight is possible from minute to minute. We find signals that may serve as such a diagnostic in the raw output of the dGPS systems that we tested, but they are not currently available to the pilot.

3. Develop alternative positioning technology

Lastly, other sources of position determination may close the gap that currently hinders autonomous UAV inspection flights. Compact sonar detectors are available with specifications that claim accurate distance measurement up to about 20 feet. Lidar has a far greater inherent range, but compact units with suitable size, power, and spatial resolution are not assured. In general, there is a tradeoff: a lidar system has a) small size and power consumption, or b) high spatial resolution, but not both. Radar, similarly, is inherently capable, but so far no compact units are in widespread use. The hardware required for visual ranging using stereo camera streams or a time sequence of images (phodar) is quite compact, but the real-time computation needed to make it useful is complex and requires very powerful processors. It may be possible in 2017 using onboard processors.

Multiple sensors

Our early designs for airborne compact UV sensors used three sensors on each side of the UAV, so that a corona source was tracked during approach, at closest separation, and after the UAV flew past (Figure 18). This horizontal, fore-mid-aft design offered signal validation and directional information at a low cost - each sensor added only modestly to the cost of a UAV. We used a downward facing vertical array design in a feasibility study to measure from two conductors simultaneously with a UAV flying over them (Appendix 3). Given the arbitrary pose angles that may arise in some of the vertical standoff UAV positions sketched in Figure 17, we expect that an array of multiple onboard sensors is the most agile and productive approach at this stage of research.
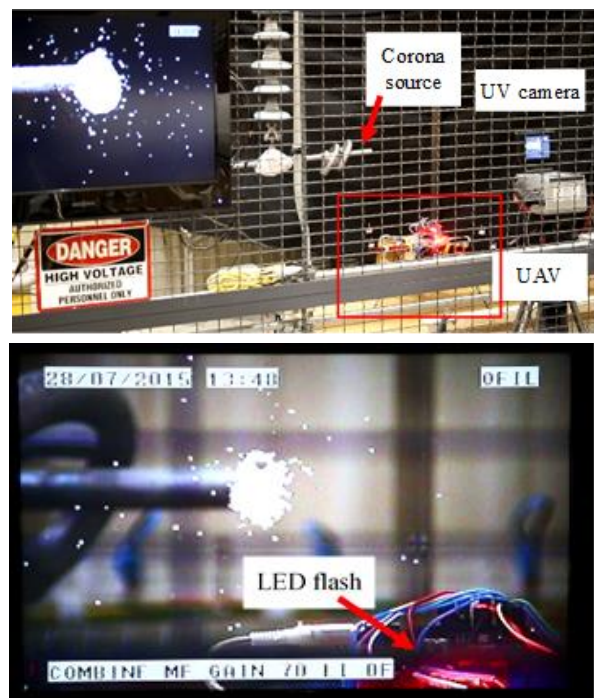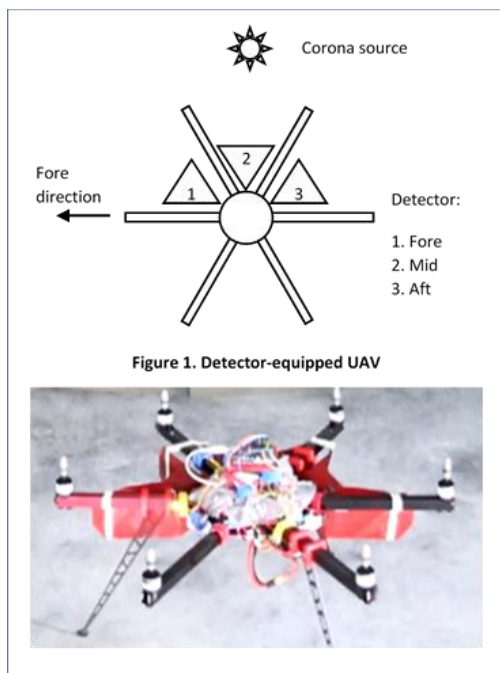
Figure 18. Multi-sensor payload design, used to calibrate the first generation sensor. Left: concept and prototype. Right: calibration to 100 kV corona at the Electric Power Research Institute, July, 2015 [23]. The top right image shows the calibration setup, and the bottom right image shows view through a commercial corona camera. The corona is indicated by white spots overlaid on a visible-band image. The red LED flash indicates UV detection. *UV imagery source: Electric Power Research Institute, Charlotte, NC*

Conclusion

In this report, we documented test and measurement flights of a UAV, equipped with a low-cost UV sensor, at two de-energized high-voltage structures. In the measurement flights, the sensor signal was verified with a ground-based commercial corona camera, and the UAV position was monitored on a local ground station laptop. Simultaneously, the laptop transmitted the UAV position to a remote server that tracked it in the US air space.

Incidental navigation and sensing technology gaps were reviewed and future improvements to mitigate them were recommended. One technology gap that prevents precision autonomous UAV inspection flights is positional accuracy. Neither sGPS nor dGPS can close the gap with systems that cost less than the UAV. The two low-cost differential GPS systems tested are small enough to fly on an under-55-lb UAV, but fail intermittently; this can result in abrupt position changes during the UAV flight.

Other methods for position determination may close the gap that currently hinder precision autonomous UAV inspection flights. Compact sonar detectors are available with specifications that claim accurate distance measurement up to about 20 feet, but their spatial resolution is quite coarse (typical a single distance). Lidar has a far greater inherent range, but compact units with suitable size, power, and spatial resolution are not assured. Locating and avoiding wires is particularly challenging for current compact LIDAR. In general, there is a tradeoff: a lidar system has a) small size and power consumption, or b) high spatial resolution, but not both. Radar, similarly, is inherently capable, but so far no compact units are in widespread use. The hardware required for visual ranging using stereo camera streams or a time sequence of images (phodar) is quite compact, but the real-time computation needed to make it useful is complex and requires very powerful processors which are currently not compact enough for onboard deployment.

Increasing the range of onboard UV sensors would lessen the need for precision position determination. If the standoff distance can be doubled from 12 feet to 24 feet with compact optics, then sGPS would be sufficiently accurate. With a sensitivity improvement high enough to allow a safe standoff distance using affordable positioning technology, a fleet of UAVs equipped with compact UV sensors could serve as an autonomous detection capability that enables a self-diagnosing power grid.

References

1. Blanks, Mark. "UAS Applications." *Introduction to Unmanned Aircraft Systems* (2016): 19.
2. Knight, Rence. "The Power of UAS." Inside Unmanned Systems. January-February 2017: 31
3. Ito, Robert. "Unmanned Aircraft Systems Pass Field Tests with Flying Colors." *Epri Journal* November-December 2017: 16.
4. Wolf, Gene. "The Drone Advantage." Transmission and Distribution World. Vol. 68 No. 4, April 2016: 106
5. Matikainen, Leena, et al. "Remote sensing methods for power line corridor surveys." *ISPRS Journal of Photogrammetry and Remote Sensing* 119 (2016): 10-31.
6. Menendez, Oswaldo A., Marcelo Perez, and Fernando A. Auat Cheein. "Vision based inspection of transmission lines using unmanned aerial vehicles." *Multisensor Fusion and Integration for Intelligent Systems (MFI), 2016 IEEE International Conference on*. IEEE, 2016.
7. Prevot, Thomas, et al. "UAS traffic management (UTM) concept of operations to safely enable low altitude flight operations." 16th AIAA Aviation Technology, Integration, and Operations Conference. 2016.
8. Warashina, Hidenaga. "Ultraviolet detector", US Patent 5959301 A, Sep 28, 1999

9. Engelhaupt, Darell E., et al. "Autonomous long-range open area fire detection and reporting." Defense and Security. International Society for Optics and Photonics, 2005.

10. Engelhaupt, Darell Eugene. "Optical flame detection system and method." U.S. Patent No. 7,541,938. 2 Jun. 2009.

11. Kim, Youngseok, and Kilmok Shong. "The characteristics of UV strength according to corona discharge from polymer insulators using a UV sensor and optic lens." *IEEE transactions on power delivery* 26.3 (2011): 1579-1584.

12. Kim, Young-Seok, and Kil-Mok Shong. "Measurement of corona discharge on polymer insulator through the UV rays sensor including optical lens." Solid Dielectrics (ICSD), 2010 10th IEEE International Conference on. IEEE, 2010.

13. Meier, Lorenz, Dominik Honegger, and Marc Pollefeys. "PX4: A node-based multithreaded open source robotics framework for deeply embedded platforms." Robotics and Automation (ICRA), 2015 IEEE International Conference on. IEEE, 2015.

14. Schubert, Matthew, and Andrew J. Moore. "Morphological processing of ultraviolet emissions of electrical corona discharge for analysis and diagnostic use." *Applied Optics* 55.7 (2016): 1571-1572.

15. Rymer, Nicholas, Andrew J. Moore, Matthew Schubert, and James Hubbard. "Directional UV Detection for UAV Power Line Inspection." Online video clip. YouTube, 14 September 2015. Web. 8 March 2017. https://youtu.be/GPePalYC28M

16. Parkinson, Bradford W., and Per K. Enge. "Differential gps." *Global Positioning System: Theory and applications.* 2 (1996): 3-50.

17. Civil Report Card On GPS Performance Nov 2016. (2016, December). Retrieved March 15, 2017, from http://www.nstb.tc.faa.gov/reports/ReportCards/2016_11.pdf

18. Hamamatsu Flame Sensor UV TRON, Hamamatsu Photonics K.K., Electron Tube Center, Shimokanzo, Toyooka-village, Iwata-gun, Shizuoka-ken, 438-0193, Japan

19. Moore, Andrew J., Matthew Schubert, and Nicholas Rymer. "Drone senses power line corona while tracked in U.S. airspace: NASA-Dominion UAV Flight Test with Compact Corona Sensor and UTM Tracking." Online video clip. YouTube, 31 March 2017. Web. 31 March 2017. https://youtu.be/8shsiM-PMjs

Appendix 1. Inventory of Flights

Table 3. Inventory of flights

Test flights									
Date	Location	Flight	Description	UV Plot	Flight path	UV Image	Visible Image	UTM path	UTM boundary
Monday, Nov 7	Substation	S1_1	1st manual flight		✓				
		S1_2	1st auton. flight	✓	✓		✓		
		S1_3	2nd auton. flight	✓	✓		✓		
	Tower	T1_1	1st manual flight		✓				
		T1_2	1st auton. flight, aborted						
		T1_3	2nd auton. flight, aborted	X	✓				
		T1_4	3rd auton. flight, aborted	X	✓				
Tuesday, Nov 8	Substation	S2_1	1st manual flight	✓	✓		✓	✓	
		S2_2	1st auton. flight, aborted	✓				✓	
	Tower	T2_1	1st manual flight		✓				
		T2_2	1st auton. flight, aborted					✓	
		T2_3	2nd auton. flight, aborted					✓	
Measurement Flights									
Date	Location	Flight	Description	UV Plot	Flight path	UV Image	Visible Image	UTM path	UTM boundary
Tuesday, Nov 8	Substation	S2_3	2nd auton. flight		✓			✓	
		S2_4	3rd auton. flight	✓	✓			✓	
		S2_5	4th auton. flight	✓	✓	✓	✓	✓	✓
	Tower	T2_4	3rd auton. flight	✓	✓	✓	✓	✓	✓

Appendix 2. Experimental Equipment

1. Right (Starboard) UV Sensor
2. Pixhawk GPS Antenna/Compass
3. UV & Telemetry Beaglebone
4. Left (Port) UV Sensor
5. Safety Relay

(Not visible)
Pixhawk autopilot
Arduino UV sensor processor
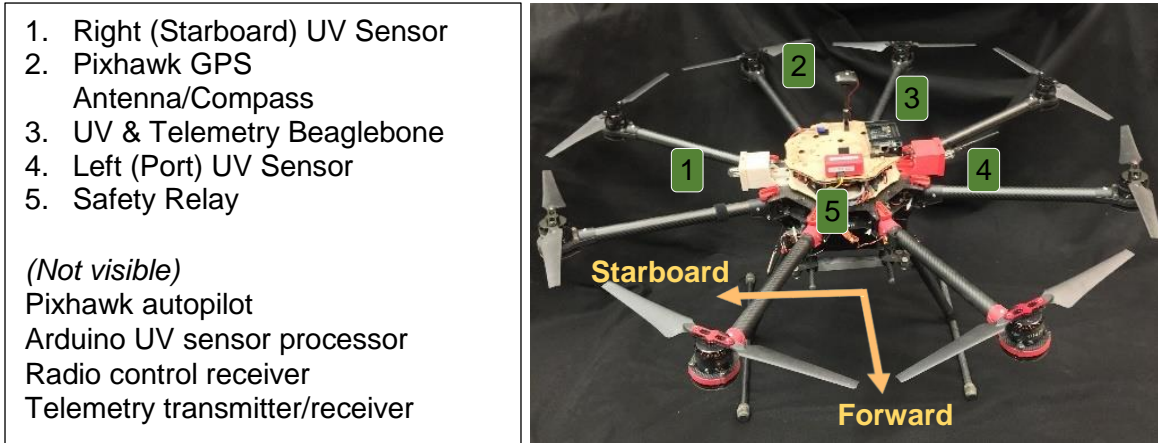Radio control receiver
Telemetry transmitter/receiver

Figure 19. The aircraft FA3WEANXWH was used in all flights. It is comprised of a DJI S1000 frame, a Pixhawk autopilot, three onboard single-board computers, and custom sensing and telemetry electronics.
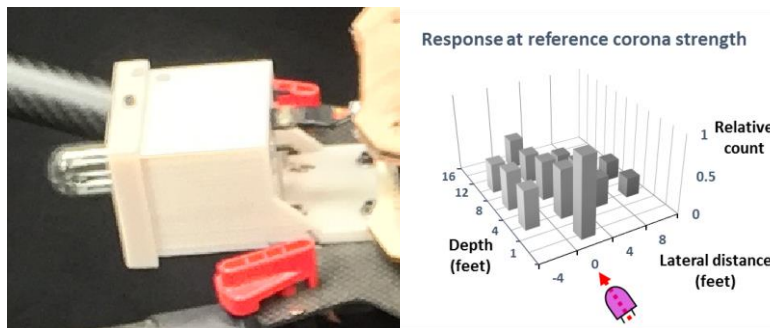

Figure 20. Left: The Hamamatsu R13192, which can sense a 100 kV corona at a distance of ~ 12 feet. Center: Sensitivity plot of R13192.

The Electro-Technic Products BD-20A High Frequency Generator was used to produce corona in these experiments. The following were used for image capture and computing: UVolle-VC corona camera, Canon EOS 1D Mark II visible camera, Dell Precision M6700 laptop (running Centos Linux), Panasonic CF-54 Toughbook (running Windows 8). The following were used for communications and control: Spektrum 18 channel transmitter, 3DR 915 MHz telemetry link, Verizon Jetpack LTE/Wifi hotspot.

Component	Software	Version
Pixhawk autopilot	Arducopter	3.3.3
Ground station Dell laptop	Centos Linux	6.8
Ground control (operation)	APMPlanner	2.0.19-rc4
Ground control (configuration)	QGroundcontrol	StableV3.0
Telemetry monitor	MavProxy	1.4.42
Power distribution voltage control	Castle Link CC BEC Pro	3.62.00

Source	Frequency	Purpose
3DR Radio	915MHz (Ch. 1)	Ground station command and control
Spektrum	2.4GHz	R/C command and control

Figure 21. Software package versions (top) and radio frequencies (bottom) used in the flights

Table 4. Custom mission software

Custom Software	Functionality	Substrate	Origin
Commbox	On-board: gather UV sensor data and convert into Arducopter/Mavlink telemetry protocol, forward commands to autopilot, and forward telemtry to ground station. On ground station: receive UV and other telemetry, and log UV data to separate file.	Onboard Beaglebone Black	NASA Langley A2I group
UV_Pulse	On-board: read from each UV sensor, encode pulse count and send to Commbox	Onboard Arduino Uno	NASA Langley A2I group
UTM client	Ground-to-server: gather UAV location estimate from groundstation telemetry and post to UTM server	Panasonic Toughbook	NASA Ames UTM group
RelAlt	Postprocessing: script to substitute relative altitude (instead of absolute altitude) before export from telemetry log to KML, for rendering in Google Earth	Any	NASA Langley A2I group
Icarous	On-board: compare autopilot location estimate to preplanned flight path and correct trajectory as needed to return to flight path. *Installed but not activated.*	Onboard Beaglebone Black	NASA Langley Icarous group
Geofence uploader	Ground-to-air: read geofence and obstacle field polyhedra and send to Icarous. *Installed but not activated.*	Groundstation Dell	NASA Langley A2I group

Appendix 3. Example flight geometry

Figure 22 and Figure 23 illustrate an example flight geometry with the following assumptions:
1) No lens
2) 3rd generation UV sensor with manufacturers' sensitivity estimate
3) Spatial sensitivity profile the same as the 2nd generation sensor
4) Maximum detection distance (as determined from a 100kV test) is 12'

With the conservative assumption that it takes one second to store and geostamp the UV sensor telemetry, the top flight speed is 14 feet per second (9.5 miles per hour).
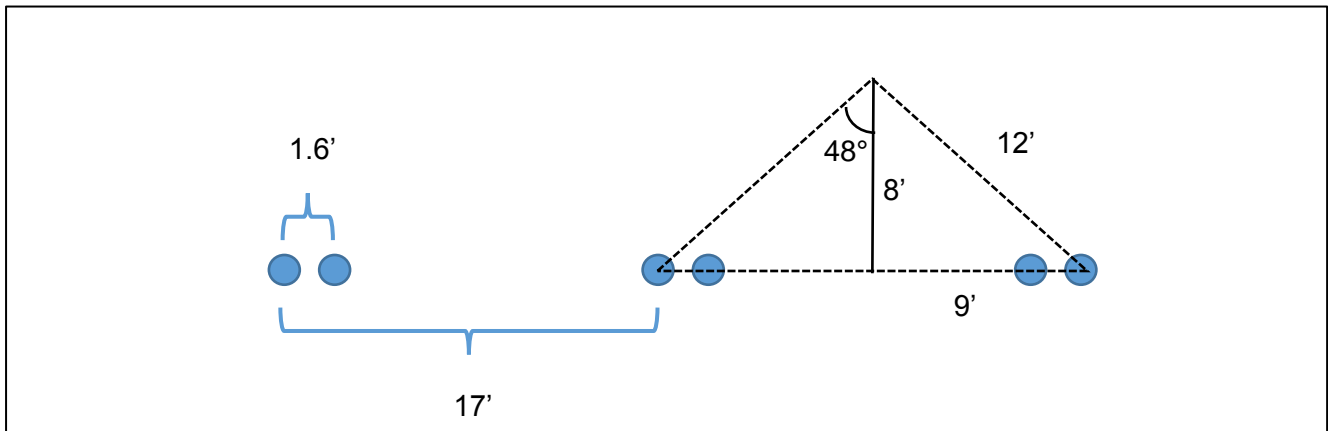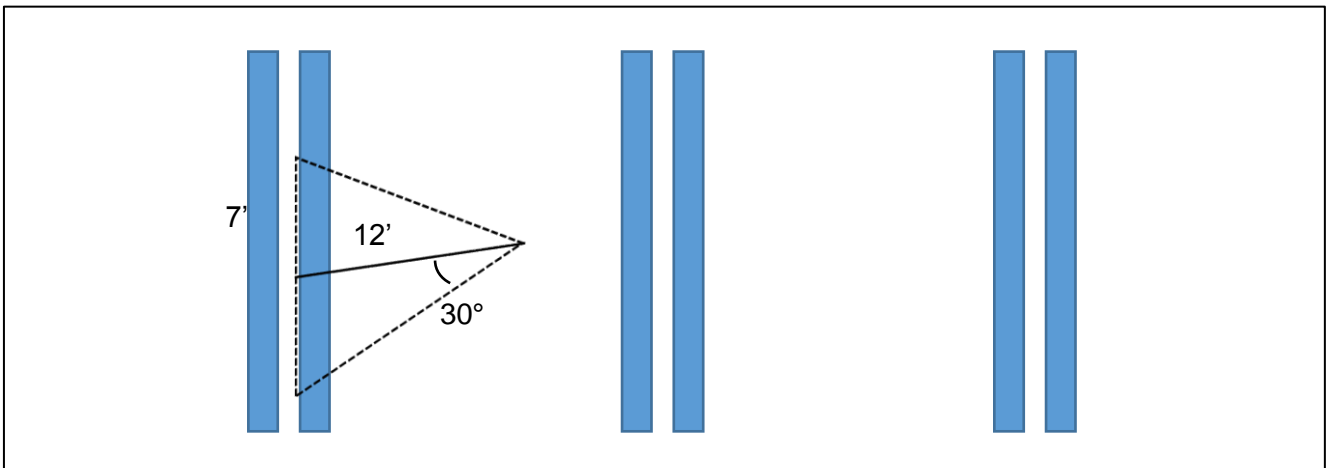

Figure 22. Example flight geometry for transmission line with conductors separated by 17 feet (view along the conductors). Due to the maximum sensing distance of twelve feet, two passes of the UAV carrying two sensors are needed. At an eight foot height above the midline between 2 phases is, the sensors should be mounted 48° from vertical.

Figure 23. Example flight geometry for transmission line with conductors separated by 17 feet (view from above, looking down at the conductors). According to the sensitivity plots from the sensor manufacturer (not shown), each sensor will be at 95% sensitivity 30° in front of and behind the current location. For a standoff distance of twelve feet, this corresponds to a fourteen foot field of view.

REPORT DOCUMENTATION PAGE

1. REPORT DATE (DD-MM-YYYY)	2. REPORT TYPE	3. DATES COVERED (From - To)
01-05-2017	Technical Memorandum	

4. TITLE AND SUBTITLE	5a. CONTRACT NUMBER
Autonomous Inspection of Electrical Transmission Structures with Airborne UV Sensors - NASA Report on Dominion Virginia Power Flights of November 2016	5b. GRANT NUMBER
	5c. PROGRAM ELEMENT NUMBER

6. AUTHOR(S)	5d. PROJECT NUMBER
Moore, Andrew J.; Schubert, Matthew; Rymer, Nicholas	5e. TASK NUMBER
	5f. WORK UNIT NUMBER
	154692.02.70.07.02

7. PERFORMING ORGANIZATION NAME(S) AND ADDRESS(ES)	8. PERFORMING ORGANIZATION REPORT NUMBER
NASA Langley Research Center Hampton, VA 23681-2199	L-20808

9. SPONSORING/MONITORING AGENCY NAME(S) AND ADDRESS(ES)	10. SPONSOR/MONITOR'S ACRONYM(S)
National Aeronautics and Space Administration Washington, DC 20546-0001	NASA
	11. SPONSOR/MONITOR'S REPORT NUMBER(S)
	NASA-TM-2017-219611

12. DISTRIBUTION/AVAILABILITY STATEMENT

Unclassified
Subject Category 01
Availability: NASA STI Program (757) 864-9658

13. SUPPLEMENTARY NOTES

14. ABSTRACT

The report details test and measurement flights to demonstrate autonomous UAV inspection of high voltage electrical transmission structures. A UAV built with commercial, off-the-shelf hardware and software, supplemented with custom sensor logging software, measured ultraviolet emissions from a test generator placed on a low-altitude substation and a medium-altitude switching tower. Since corona discharge precedes catastrophic electrical faults on high-voltage structures, detection and geolocation of ultraviolet emissions is needed to develop a UAV-based self-diagnosing power grid. Signal readings from an onboard ultraviolet sensor were validated during flight with a commercial corona camera. Geolocation was accomplished with onboard GPS; the UAV position was logged to a local ground station and transmitted in real time to a NASA server for tracking in the national airspace.

15. SUBJECT TERMS

Air traffic; Autonomous flight; Electric power; Infrastruvture Inspection; UAV; UTM; UV sensing

16. SECURITY CLASSIFICATION OF:			17. LIMITATION OF ABSTRACT	18. NUMBER OF PAGES	19a. NAME OF RESPONSIBLE PERSON
a. REPORT	b. ABSTRACT	c. THIS PAGE			STI Help Desk (email: help@sti.nasa.gov)
U	U	U	UU	30	19b. TELEPHONE NUMBER (Include area code) (757) 864-9658